Pharm Res (2011) 28:2808–2819
DOI 10.1007/s11095-011-0530-6

RESEARCH PAPER

Development of Novel Peptides for Mitochondrial Drug Delivery: Amino Acids Featuring Delocalized Lipophilic Cations

Shana O. Kelley • Kelly M. Stewart • Rida Mourtada

Received: 21 February 2011 / Accepted: 29 June 2011 / Published online: 11 August 2011

ABSTRACT

Purpose To create a new class of mitochondria-penetrating peptides (MPPs) that would facilitate drug delivery into the organelle through the inclusion of delocalized lipophilic cations (DLCs) in the peptide sequence.

Methods We synthesized two novel amino acids featuring DLCs and incorporated them into peptides. Systematic studies were conducted to compare peptides containing these residues to those with natural cationic amino acids. Diastereomers were compared to determine the most advantageous arrangement for these peptides. Peptide lipophilicity, cellular uptake and mitochondrial specificity were compared for a variety of peptides.

Results Synthetic DLC residues were found to increase mitochondrial localization of MPPs due to higher overall hydrophobicity. MPP stereochemistry was important for cellular uptake rather than subcellular localization. This study reaffirmed the importance of uniform overall charge distribution for mitochondrial specificity.

Conclusions DLCs can be incorporated into synthetic peptides and facilitate mitochondrial drug delivery. Lipophilicity and charge distribution must be carefully balanced to ensure localization within mitochondria.

Electronic Supplementary Material The online version of this article (doi:10.1007/s11095-011-0530-6) contains supplementary material, which is available to authorized users.

S. O. Kelley • K. M. Stewart
Department of Biochemistry, Faculty of Medicine
University of Toronto
Toronto M5S 3M2, Canada

S. O. Kelley (✉) • R. Mourtada
Department of Pharmaceutical Sciences
Leslie Dan Faculty of Pharmacy, University of Toronto
Toronto M5S 3M2, Canada
e-mail: shana.kelley@utoronto.ca

KEY WORDS cell-penetrating peptides · drug delivery · mitochondria · mitochondria-penetrating peptides

ABBREVIATIONS

CPP	cell-penetrating peptide
DLC	delocalized lipophilic cation
MPP	mitochondria-penetrating peptide

INTRODUCTION

The class of short cationic peptide sequences referred to as cell-penetrating peptides (CPPs) translocate plasma membranes and are able to promote cellular internalization of diverse bioactive cargo molecules (1,2). For example, these cationic peptides are capable of delivering large globular proteins (e.g. 150 kDa immunoglobins and 465 kDa β-galactosidase) (3), 45 nm magnetic nanoparticles (4), and various small molecule therapeutics (5,6). Despite the formidable challenge for promoting intracellular accumulation of large or hydrophobic cargos, some of these systems have demonstrated clinical potential. In particular, a topically administered cyclosporine CPP-conjugate was able to penetrate human and mouse skin to effectively inhibit cutaneous inflammation. CPP-derivatized superparamagentic nanoparticles have allowed for the *in vivo* tracking of progenitor cells by high-resolution magnetic resonance imaging (4,6).

In order to optimize CPPs for delivery applications, various studies have been carried out to thoroughly investigate the critical features and relevant chemical modifications that enhanced a particular aspect of their delivery properties. For example, synthetic sequences, inspired by a survey of the natural-derived sequences, were

designed to increase the cellular internalization of these molecules (7). In addition, exchanging the amide backbone for a peptoid (7), carbamate (8,9), β-amide (10), or alternative chemical scaffold (11,12) resulted in enhanced proteolytic stability and even stronger cellular uptake. Furthermore, the overall chirality of the molecules was examined in an effort to increase proteolytic stability and cellular uptake for the CPPs (7,13). From this work, it is evident that the chemical structure of these peptides does play a role in their biological properties and that these types of modifications can result in enhanced versions of the delivery vector.

A novel class of cationic peptides that efficiently traverse plasma membranes of multiple cell types and also traverse mitochondrial membranes was discovered recently (14). A series of mitochondria-specific peptides, referred to as mitochondria-penetrating peptides (MPPs), were then later characterized (15). Modifying the chemical properties, such as overall lipophilicity, or charge distribution of MPPs was shown to have a direct effect on mitochondrial membrane permeability and, hence, subcellular localization of MPPs (15,16). It was clear that slight adjustments to the chemical properties or structure of these novel peptides strongly influenced the cellular characteristics, emphasizing the intimate relationship between the chemistry and biology of MPPs. In follow-up investigations, the MPPs were explored as vehicles for small-molecule delivery in mammalian cells (16–18). Recently, MPPs have been used to deliver the DNA alkylating drug chlorambucil (Cbl). Interestingly, MPP-Cbl conjugates were shown to evade cellular resistance mechanisms typically used by cancer cells to diminish drug toxicity (17). Moreover, additional studies have shown that mitochondrial drug delivery can enhance the activity of antibacterial agents by sequestering a drug away from its target and mitigating toxic effects in human cells (18).

The MPPs originally characterized were composed of sequences displaying alternating cationic and hydrophobic residues. To facilitate the use of these peptides as drug delivery vectors, it could be advantageous to combine cationic character and hydrophobicity into a single amino acid residue. Merging these two characters into a single moiety, as in triphenyphosphonium ions, is known to impart mitochondriotropicity onto delivery vectors (19). Delocalized lipophilic cations (DLCs), which display hydrophobicity compatible with passage through membranes and a dispersed charge that does not prohibit membrane immersion in response to a potential gradient, are well-known mitochondrial localizers (20–22), but amino acids displaying this type of functional group are not currently available. This report details the synthesis of such residues and their behavior in MPPs.

MATERIALS AND METHODS

Acetic anhydride, Dimethylsulfoxide (DMSO), *N*,*N*-Diisopropylethylamine (DIPEA), 3-methylbenzothiazole-2-thione, iodomethane, methanol (MeOH), diethylether (Et_2O), 4-methylquinoline, 6-bromohexanoic acid, dichloromethane (DCM), acetone (Me_2CO), triethylamine (TEA), trifluoroacetic acid (TFA), triisopropylsilane (TIS), pyridine, 1-chloro-2-4-dinitrobenzene, nitromethane, iodopropane, iodohexane, fetal bovine serum, Sytox Red, and 1-octanol were purchased from Sigma-Aldrich (St. Louis, MO). MBHA Rink amide resin and Fmoc-Lys(Dde)-OH were purchased from NovaBiochem (Hohenbrunn, Germany). All other Fmoc-protected amino acids (Fmoc = 9-fluorenylmethyloxycarbonyl) were purchased from Advanced ChemTech (Louisville, KY), except for Fmoc-D-4-Pyridylalanine-OH (Fmoc-D-Pal-OH) and Fmoc-Pyridylalanine-OH (Fmoc-Pal-OH), which were purchased from SyntheTech (Albany, OR). *O*-(benzotriazol-l-yl)-*N*,*N*,*N*′,*N*′-tetramethyl-uronium hexafluorophosphate (HBTU), 4-methylmorpholine (NMM) in N,N-dimethylformamide (DMF) and 20%(v/v) piperidine in DMF were obtained from Protein Technologies Inc. (Tucson, AZ). Acetonitrile (MeCN) was purchased from Caledon Labs (Georgetown, ON). Minimum essential medium (MEM-α), MEM-α [no phenol red], Iscove's Media, Dulbecco's Phosphate-Buffered Saline (PBS), 0.25% Trypsin-EDTA and Mitotracker Deep Red 633 were obtained from Invitrogen (Carlsbad, CA). The Cell-Counting Kit (CCK8) reagent was purchased from Dojindo (Rockville, MD).

Peptide Synthesis

Solid-phase synthesis was performed at a 50 μmole scale on MBHA Rink amide resin (0.6–0.7 mmol/g, 100–200 mesh) using a Prelude automated peptide synthesizer (Protein Technologies Inc.). Couplings were performed with 4 equivalents of Fmoc-protected *d* or *l*-amino acids, HBTU (4 equiv.) and NMM (8 equiv.) in DMF for 1 h. The following orthogonally protected monomers were used: Fmoc-D-Arginine(Pbf)-OH, Fmoc-D-Lysine(Boc)-OH, Fmoc-Cha-OH (cyclohexyl alanine), Fmoc-Alanine-OH, Fmoc-D-Pal-OH,and Fmoc-Pal-OH. Due to poor solubility in DMF, the protected pyridylalanine (Pal) monomers were solubilised in a 70%/30% mixture of DMSO/DMF. Double couplings were performed for all arginine residues. Between couplings, the Fmoc group was removed with piperidine (20% v/v) in DMF (2×10 min), and the resin was washed with DMF (3×5 min). In order for the peptides to be amenable for microscopy and flow cytometry studies, the deprotected N-termini of the completed peptides were conjugated to a carboxy-derivatized thiazole orange fluorophore (*to)* (2-[[1-(5-carboxypentyl)-4(1H)-quinolinylidene]

methyl]-3-methyl-benzothiazolium bromide) (3 equiv) with HBTU (3 equiv) and DIPEA (3 equiv) for 3 h.

The derivatized thiazole orange dye was synthesized as described previously (23). Briefly, 3-methylbenzothiazole-2-thione (2.77 g) and iodomethane (10.8 g) were combined and heated to 45°C for 4 h. The resulting solid was then dissolved in MeOH, filtered and washed with Et_2O to afford 3-methyl-2-(methylthio)-benzothiazolium iodide (**7**) as a white solid (Fig. S1). 4-methylquinoline (1.50 g) and 6-bromohexanoic acid (2.26 g) were combined and heated to 125°C for 4 h. The reaction was cooled to room temperature, and the brown residue was dissolved in MeOH and concentrated *in vacuo*. The residue was then dissolved in DCM, cooled to 0°C and washed with Me_2CO to afford 1-(5-carboxypentyl)-4-methyl-quinolinium bromide (**8**) as a light grey solid (Fig. S1). Stoichiometric equivalent amounts of **7** and **8** were dissolved in DCM to which TEA (2.2 equiv.) was added. The resulting red mixture was stirred at room temperature for 24 h, filtered and washed to afford 2-[[1-(5-carboxypentyl)-4(1H)-quinolinylidene]methyl]-3-methyl-benzothiazolium bromide as a red solid (Fig. S1). The product was confirmed by ^{1}H NMR and mass spectrometry as described previously.

The peptide conjugates were detached from the resin, and all amino acid side chain protecting groups were removed in a single step by adding 95/2.5/2.5% TFA/H_2O/TIS v/v to the resin for 2 h. The solvent was allowed to drip slowly through the resin bed and collected into a 50 mL conical tube. After washing the resin with ~5 mL of MeOH, chilled Et_2O (40 ml) was added, and the resulting crude mixture was centrifuged to isolate the peptide. The resulting solid was dissolved in TFA/H_2O (0.1% v/v) and purified by reverse-phase HPLC with a Shimatzu preparative LC-8A series HPLC equipped with a diode array detector using a preparative column (*Zorbax 300SB C-18,* 7 µm, 21.2×250 mm) at a flow rate of 10 mL/min. The mobile phases were MeCN/0.1%TFA and H_2O/0.1% TFA, and the gradient was 0.8%/min. Purity of the resultant product was assessed by an analytical Agilent 1100 series HPLC using a linear solvent gradient from 5% to 100% B over 60 min (solvent A=0.1% TFA in H_2O; solvent B=0.1% TFA in MeCN) with an analytical column (Varian C18, 5 µm, 250×4.using a mm) at a flow rate of 1.0 mL/min; retention times are reported in the Supplementary Material. Purity of all peptides used in this study was greater than or equal to 95%. ESI mass spectrometry was used to confirm the identity of the conjugates.

Synthesis of Peptide Displaying k_π Residues (1c)

Using the solid-phase peptide synthesis protocol described above, the C-terminal amidated, fluorophore-labeled peptide with the sequence Fx-k-Fx-k-Fx-k was synthesized and dried after cleavage from the resin and Et_2O precipitation. The Zincke reaction to convert the primary amines into pyridyl salts was completed as described previously (24,25). The peptide was dissolved in MeOH (4°C) and added, dropwise, to a chilled solution of Zincke salt (5 equiv. per amine) in MeOH. The solution was transferred to a 25 mL dry round-bottom flask fitted with a Liebig condenser. After the addition of excess TEA (3 equiv.), the dark red solution was refluxed for several days until the reaction was complete, as monitored by ESI Mass Spectrometry analysis. The main product intermediate, as detected by ESI Mass Spectrometry, was *to*-(Fx-k_π)$_2$-Fx-k (Fig. S2a). Once the reaction was completed (approximately 4 days), the peptide was precipitated by the addition of chilled Et_2O and purified by HPLC as described above. The Zincke salt used in these reactions was synthesized as described previously (24,25). Briefly, pyridine (2 equiv.) was added to 1-chloro-2-4-dinitrobenzene (3 equiv.) in DMF and heated to 100°C. The mixture was stirred for 1 h, then dissolved in MeOH and precipitated in Et_2O. After washing in Et_2O, the resulting pale yellow crystals were obtained in 83% yield. (Mass spec analysis: calculated mass: 246.1 g/mol, observed mass: 246.1 g/mol.)

Synthesis of Peptides Displaying Pro-Pal Residues (1d, 1e, 2, 3, 4, 5)

Using the solid-phase peptide synthesis protocol described above, the fluorophore-labeled peptides with the sequences Fx-(D-Pal)-Fx-(D-Pal)-Fx-(D-Pal), Fx-(Pal)-Fx-(Pal)-Fx-(Pal), (D-Pal)$_6$, (D-Pal)$_3$, (A-(D-Pal)-A-(D-Pal)-A-(D-Pal) were synthesized as the starting materials for **1d**, **1e**, **2**, **3**, **4**, **5**, respectively. Either solid-phase or solution-phase alkylation reactions were used to convert the pyridine side chains into the pyridyl salt derivatives, as both methods afforded the desired product. For solution phase, the peptides were cleaved from the resin, as described above, dissolved in nitromethane with excess (~100-fold) iodopropane or iodohexane and refluxed for 48 h at 60°C behind a blast shield. The functionalized peptides were precipitated and washed extensively in chilled Et_2O. For solid-phase reactions, after peptide-synthesis and dye conjugation, the resin was suspended in ~5 mL of a solution of dry DMF and the respective iodoalkane and heated at 65°C for 48 h to allow the reaction to progress. After 48 h, the resin was extensively washed with DMF, MeOH and DCM. The functionalized peptide was cleaved from the resin as described above. Reaction intermediates, detected by ESI mass spectrometry, were mainly peptides with different levels of alkylation (Fig. S2b). After Et_2O precipitation, the isolated peptides were purified by reverse-phase HPLC as described above and confirmed by ESI mass spectrometry analysis.

Cell Culture

HeLa cells (ATCC) were cultured as subconfluent monolayers on 75 cm^2 cell culture plates with vent caps (Sarstedt, Germany) in MEM-α supplemented with 10% (v/v) fetal bovine serum in a humidified incubator (70–95%) at 37°C with 5% CO_2. Cells grown to subconfluence were enzymatically dissociated from the surface with a solution of 0.05% trypsin/0.53 mM EDTA (ethylenediaminetetraacetic acid) and plated at $15–25 \times 10^3$ cells/well 1–2 days prior to the experiment in eight-well ibi-treat μ–slides (Ibidi, Germany). For cellular uptake experiments, 1×10^5 cells/well were plated in a 12-well plate 1 day prior to the experiment. These conditions produced a monolayer at subconfluence for the experiments.

Confocal Fluorescence Microscopy

Images were acquired with an inverted Zeiss LSM 510 confocal microscope using a 63x C-APO (Zeiss) water immersion lens (NA=1.2). For intracellular localization studies, the culture medium was removed, and the cells were washed in phosphate-buffered saline (PBS), pH 7.4. The cells were incubated with 1–50 μM conjugate in serum-free MEM-α [no phenol red] for 60 min. Cells were washed twice with serum-free MEM-α. After washing, serum-free media was added, and the slides were placed on ice. Images were taken immediately to minimize cell toxicity. A laser excitation at 488 nm was used, and emission was collected with a long pass filter at 505 nm. Differential interference contrast (DIC) images were also acquired.

Colocalization Analysis of Peptide Conjugates

For all colocalization studies, Mitotracker Deep Red 633 was added in the last 15 min of the incubation to achieve a final concentration of 50 nM–100 nM. Images were taken as described above, with an excitation wavelength of 488 nm for visualization of the *to*-labeled peptides, which were passed through an HFT 488 and NFT 490 filter. Emission was collected with a band pass filter at 505–550 nm. For visualization of Mitotracker Deep Red 633 nm, a HeNe laser 633 nm was passed over a HFT 488/543/633, and emission was collected with a long pass filter at 560 nm. For all colocalization studies, DIC images were taken along with both fluorescence channels.

The fluorescence images were analyzed with Colocalizer Pro software program to determine Pearson's coefficient (Rr), and values reported are average values obtained for individual representative cells (~30 cells) over multiple experiments (≥3 days). The background was subtracted from the images with a manually selected region of interest. Mitotic and unhealthy cells, as assessed by DIC, were excluded from analysis. Because large differences in signal intensity between the two fluorescence channels can introduce artifacts, only cells with comparable signals from both channels were used for calculations.

Flow Cytometry

After treatments, cells were enzymatically removed from the surface of the plate with trypsin/EDTA (500 μL/well) for 10 min at 37°C. The trypsinization was quenched with 1 mL complete MEM per well. From this point on, the samples were maintained on ice or at 4°C until analysis. The samples were transferred from the wells to sterile tubes, pelleted by centrifugation (6 min at 800 × g), and resuspended in 500 mL PBS containing 5 nM Sytox Red. Samples were then analyzed by flow cytometry on a BD FACSCanto flow cytometer (BD Biosciences). A minimum of 10,000 cells were analyzed per sample. Those staining positive for Sytox Red were excluded from analysis. The fluorescence median of the live population was used for statistical analysis.

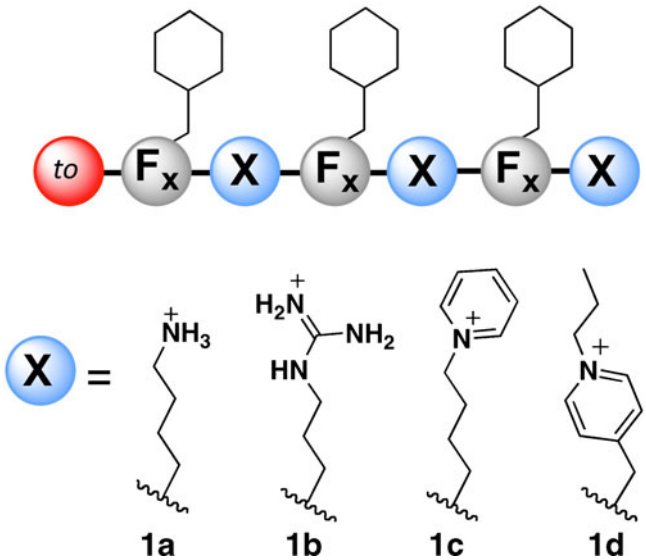

Fig. 1 Schematic of peptides used for the cation panel. Hexameric peptides were designed based on alternating hydrophobic and cationic residues to systematically examine the role of the positively charged side chain in MPP function. The hydrophobic residue cyclohexylalanine (F_x) with *l*-stereochemistry and the N-terminal dye were kept consistent throughout the panel. Peptides displaying natural amino acids *d*-lysine (**1a**) or *d*-arginine, (**1b**) in addition to synthetic amino acids *d*- k_π (**1c**) or *d*-*propal* (**1 d**), were synthesized. The fluorophore thiazole orange (*to*) was conjugated to the N-terminus so that the peptides could be detected using fluorescence microscopy and flow cytometry. See Materials and Methods for full synthesis protocols.

Octanol/Water Partitioning for Measurement of Log P

Log P values were measured via octanol partitioning by a modification of the shake-flask method as described previously. An aliquot of 100 µl of 50–300 µM peptide conjugate in Tris buffer (10 mM, pH 7.4) and 100 µL 1-octanol were added to a 0.5 mL microtube. Buffer was employed in order to measure log P of the peptide conjugates in the protonated state observed at physiological pH. The tubes were vortexed for 2 min and centrifuged for 2 min; 25 µl of each layer was removed and diluted in 100 µl 3:1 methanol:Tris or methanol: octanol for a final composition of 3:1:1 methanol: octanol:Tris. If necessary, the aqueous layer was diluted an additional 4-fold to achieve an absorbance value in the range of the detection limit of the instrument. For *to* conjugates, three dilutions were prepared per layer, 100 µL of each dilution was pipetted into a 384 well plate, and the absorbance read at 500 nm with a reference wavelength at 625 nm. The respective mean absorbance value (A_{500}) of three dilutions was calculated for each layer. The log of the absorbance ratios (e.g. A_{500} of the organic layer/A_{500} of the aqueous layer) yielded log P. This procedure was repeated a minimum of four times per conjugate to calculate the mean log P and standard deviation. All absorbance measurements used were within the linear range of the instrument.

RESULTS

Synthesis and Characterization of Novel DLC Amino Acids

We identified two different DLCs for incorporation into peptides (Fig. 1). Both are based on a pyridinium scaffold, one that features a pyridinium "cap" on a lysine residue and the other that was generated by alkylation of pyridyl alanine ("pal") with a propyl group ("pro"). Residue **1c** shown in Fig. 1 is therefore referred to as k_π, and residue **1d** is referred to as *pro-pal*. The design of these functional groups was inspired by the wealth of literature on DLCs, molecules that feature a positive charge that is effectively spread over the entire molecule through resonance stabili-

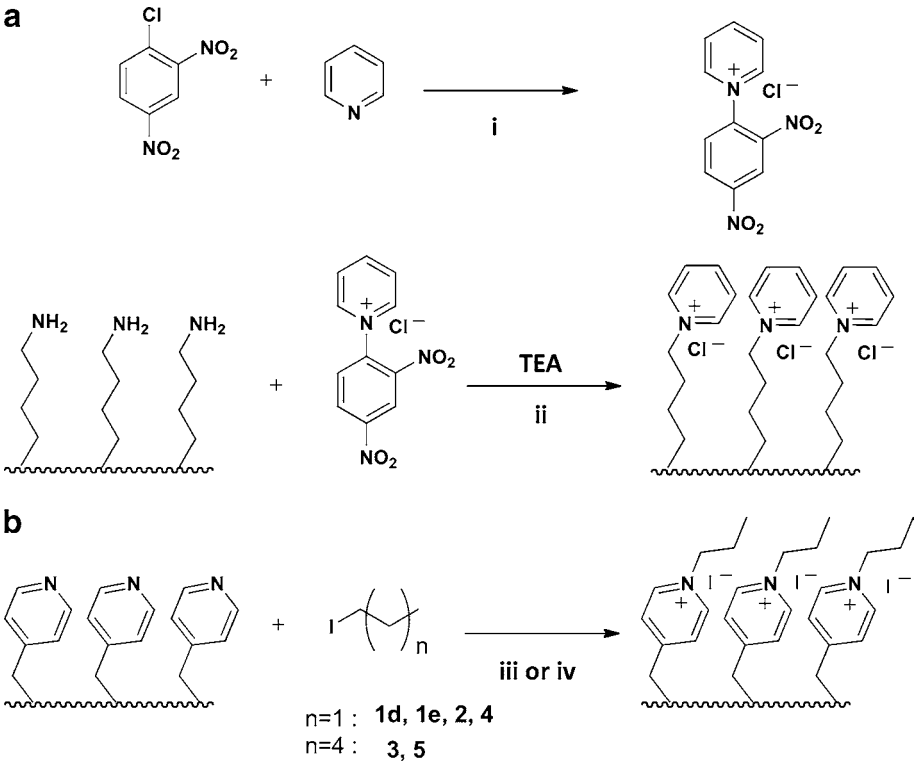

Fig. 2 Synthesis scheme for peptides displaying DLCs. All reactions were performed post-peptide synthesis to quaternize the nitrogens in all three functional groups simultaneously. (**a**) The two-step Zincke reaction was utilized to convert the primary amines into pyridinium salts for k_π residues. To prepare the Zincke salt (reaction i), 1-chloro-2-4-dinitrobenzene was refluxed in DMF in the presence of pyridine to afford the electrophilic species. In the second reaction (ii), a peptide, post-cleavage from the polymer resin and after deprotection, was refluxed in MeOH in the presence of the Zincke salt and triethylamine (TEA) to convert the lysines into k_π residues. (**b**) Peptides with pyridylalanine resides were allowed to react with an excess of iodoalkane. The reactions were carried out on solid-phase in DMF (iii) or solution-phase in nitromethane (iv) at 65°C. See Materials and Methods for full synthesis protocols. See Supplementary Material for chemical structures and mass spectrometry results.

zation. Due to the electronic structure of these permanently charged functional groups, the positive charge on the nitrogen atom is completely delocalized through the conjugated π-system. This effectively increases the radius of the ion, which lowers the free energy barrier for transferring an ion into a low dielectric medium by decreasing the enthalpic electrostatic energy component (Born energy) and increasing the favorable entropy component arising from the release of solvated water molecules (26). Since MPPs were shown to directly penetrate mitochondrial membranes (15), incorporating these synthetic amino acids into the peptide sequence allowed us to experimentally test whether delocalizing the charge on the side chains, while not over the entire molecule as in DLCs, would still offer beneficial properties for the MPPs.

The synthesis of the pyridinium salt-displaying peptides was carried out post-peptide synthesis and post-fluorophore coupling as shown in Fig. 2. To generate **1c**, the two-step Zincke reaction was utilized to convert the primary amines of the three lysine residues into pyridinium salts. While the Zincke reaction has been shown to be useful for the preparation of a single pyridyl salt group on a molecule, it is evident that this reaction is also successful for simultaneously converting the three primary amines of the peptide in a single step, since **1c** was isolated from the reaction mixture. Peptide **1d** was also prepared post-peptide synthesis through the quaternization of the pyridyl groups on the commercially available pyridyl alanine residues by heating the peptide in the presence of excess alkylating agent, iodopropane. Similarly, all three pyridines were converted to the corresponding pyridinium salts in a single step.

In order to systematically address how these new amino acids would affect the properties of MPPs, a panel of hexameric peptides was synthesized based on an alternating scaffold of hydrophobic and cationic amino acids with *l*-stereochemistry and *d*-stereochemistry, respectively (Fig. 1). The hydrophobic residue selected for this study was cyclohexylalanine (F_x), as incorporating this six-membered alkane ring into the sequence previously provided the necessary hydrophobicity needed for the selective mitochondrial accumulation of cationic peptides (15). Peptides displaying either lysine (k) or arginine (r) amino acids were synthesized in order to compare the effects of these two natural moieties, affording peptides **1a** and **1b**, respectively. Peptides displaying either k_π or *pro-pal* amino acids were synthesized in order to compare the effects of these two artificial moieties, affording peptides **1c** and **1d**, respectively.

The physiochemical properties of the peptides in the panel varied significantly, despite the fact that they each displayed an equivalent charge, length, and three F_x residues (Fig. 3). The log P of the peptides in the panel was experimentally determined in order to measure the relative lipophilicity of each molecule. In addition, measuring the retention times on a reverse-phase HPLC column allowed for another direct comparison of the relative hydrophobicities. In each measurement, peptide **1a** was more hydrophilic than **1b**, highlighting the ability of the guanidinium group to better shield the charge relative to the primary amine, thus slightly increasing the lipid partitioning of this molecule. Not surprisingly, peptide **1d** possessed a greater hydrophobicity than **1c**, likely due to the favorable interaction of the exposed alkyl chain with the stationary and octanol phases that may act as lipid surrogates. Interestingly, comparison of peptides containing natural *versus* synthetic amino acids in each measurement was not consistent. For example, the log P of peptide **1c** indicates that this peptide is the least lipophilic of the panel, while the retention suggests otherwise as **1c** elutes at a similar time to **1b**. In addition, relative to the other compounds, the hydrophobicity of **1d** was greater, as this peptide was retained more strongly on the column; however, the octanol-water partition coefficient was not significantly different from **1b**. These disparate results suggest that the pyridyl salt-containing peptides have a more favorable interaction with the stationary phase of the column that increases their apparent hydrophobicity,

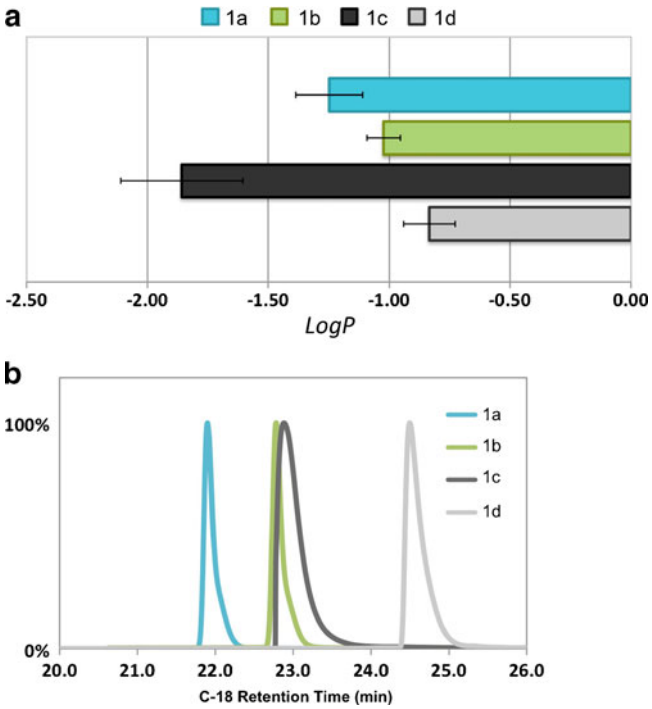

Fig. 3 Relative hydrophobicity/lipophilicity of the cation panel of peptides. (**a**) Experimentally determined octanol/water partition coefficients of peptides using the shake-flask method are displayed along with standard deviations. (**b**) Relative peptide hydrophobicity as measured by retention time on a reverse-phase C18 HPLC column. See Materials and Methods for Log P experimental design and HPLC protocol details.

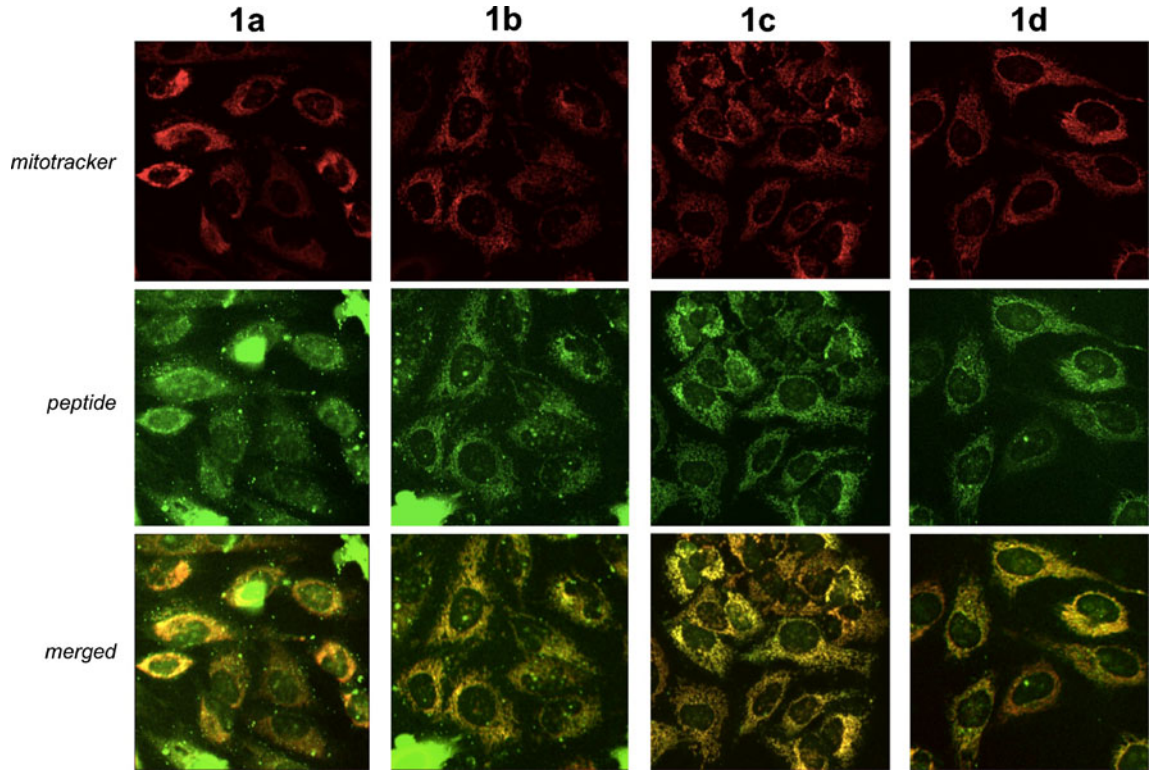

Fig. 4 Colocalization of cation panel with Mitotracker. HeLa cells were incubated with 3–8 μM peptide for 60 min and Mitotracker for the last 15 min. Images were acquired with a Zeiss LSM confocal microscope using 63x objective. Laser power, filters, and gain settings were optimized to minimize bleedthrough between fluorescence channels. See Materials and Methods for a detailed protocol. Pearson's correlation coefficients (Rr) were calculated for 30 cells for each peptide. The following average Rr values were obtained: **1a** = 0.5; **1b** = 0.7; **1c** = 0.9; **1d** = 0.8. A standard deviation of 0.1 was calculated each set of values.

as this cannot be explained by conformational effects, since the molecules are too short to adopt a particular secondary structure.

The subcellular localization profiles of each conjugate were visualized in unfixed HeLa cells after a 60-min incubation with the fluorophore-labeled peptides. Despite displaying different cationic structures, each peptide in the panel was able to access the mitochondria as seen by the characteristic fibrillar network of this organelle (Fig. 4). Nonetheless, we observed a difference in the specificity for mitochondrial localization for the peptides. For example, peptide **1a** was also seen to accumulate into the nucleus and cytoplasm. In contrast, peptides **1c** and **1d**, displaying the synthetic pyridinium salts, exhibited uniform and consistently specific mitochondrial localization, which is best illustrated in the low magnification images (Fig. S2b). Indeed, correlation coefficients calculated from colocalization images with Mitotracker showed a range of specificities (Fig. 4). From these microscopy results, it is evident that the molecular structure of the cation does play a role in the subcellular localization of the MPPs, since this trend does not directly correlate with overall hydrophobicity/lipophilicity of the peptides. Even though none of the cations abrogated mitochondrial access for the peptide, slight adjustments to the degree of specificity for the organelle were observed and highlighted the beneficial properties of the DLC-containing MPPs.

The relative cellular internalization efficiencies for the peptide panel were measured using flow cytometry to examine the effect of the cation structure on overall uptake (Fig. 5). Peptide **1b** exhibited stronger uptake relative to **1a**, suggesting that arginines promoted a stronger internalization than lysines, which has previously been shown in the literature for CPPs and their analogues (8,10,27). In addition, despite offering beneficial properties for subcellular localization, the pyridyl salt groups significantly hindered the ability of the MPPs to traverse the plasma membrane. Since the overall charge of the panel remains constant and this trend does not correlate with hydrophobicity (both of these properties are known to affect cellular uptake for peptides directly translocating lipid bilayers (7,11,28)), this suggests that the presence of the permanent charges impedes the ability of the peptide to directly traverse the bilayer. An explanation for this observation could be due to the elimination of the cationic residue's ability to participate in hydrogen bonding, since these

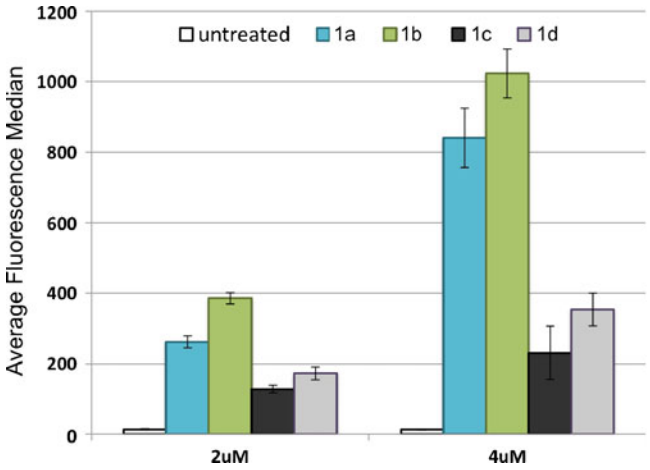

Fig. 5 Relative cellular uptake of the peptide panel. HeLa cells were incubated with various concentrations of fluorophore-labeled peptide for 60 min and analyzed by flow cytometry. The relative fluorescence median was measured for viable cells as determined from exclusion of Sytox Red signal. Standard errors from six independent trials are displayed along with the average fluorescence median. See Materials and Methods for protocol details.

interactions with the phospholipid head groups and heparan sulfate were shown to be important for the internalization of cationic peptides and their derivatives (29–32). In addition, these systematic studies confirmed that hydrogen bonding is an important initial process for cationic peptides to cross the plasma membrane, yet highlighted that this electrostatic interaction is not required for mitochondrial access. These results may indicate that MPPs utilize different biophysical mechanisms for translocating each of these biological membranes.

Investigating the Effect of Chirality of MPPs

An advantage of using artificial amino acids is their resistance to enzymatic degradation in the cell, which eliminates the need to use unnatural stereochemistry to achieve this purpose. We explored whether the peptide containing *pro-pal* exhibited different behavior when the novel amino acid was present in the *d* or *l* form. Interestingly, the diastereomer with all *l*-chiral centers (**1e**)

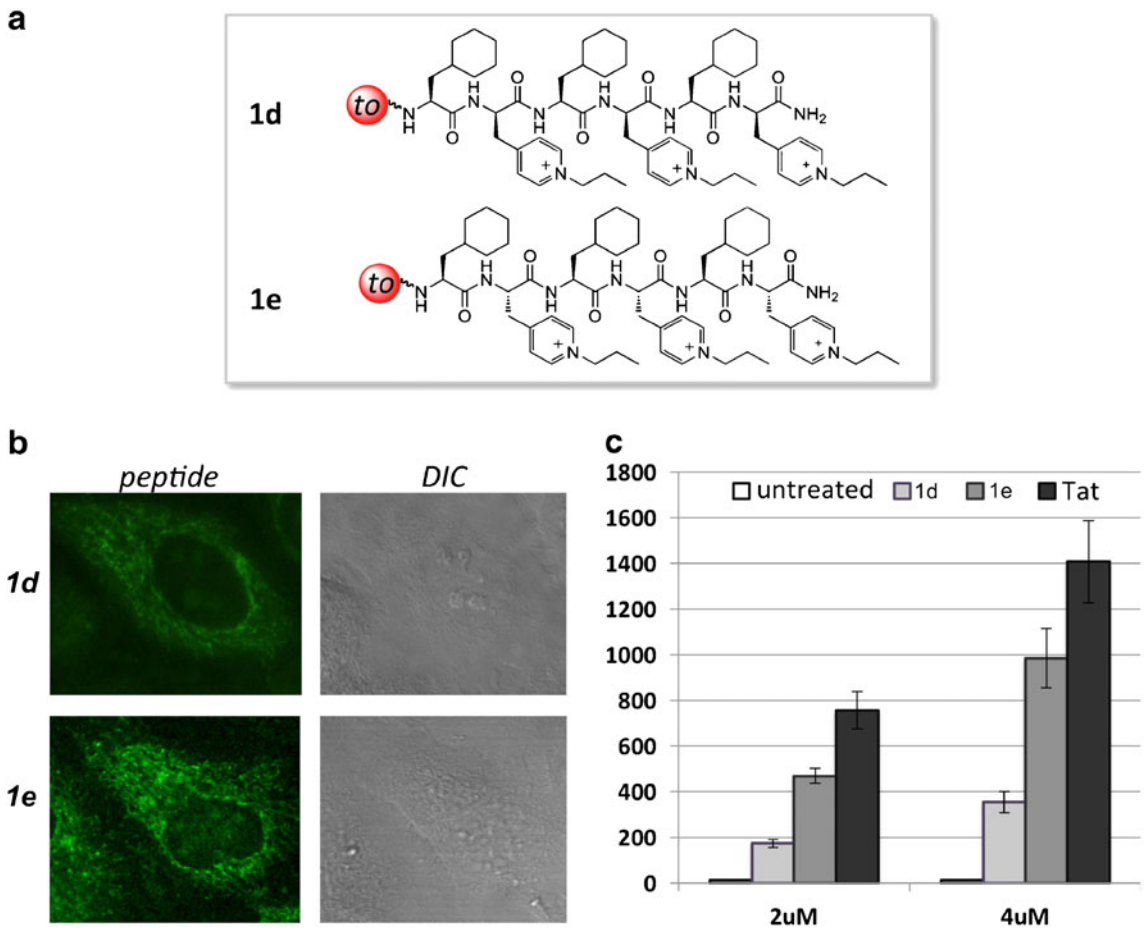

Fig. 6 Stereochemical effects of MPPs. (**a**) Schematic of fluorophore-labeled peptides used in the study with alternating hydrophobic (F_x) and cationic (*pro-pal*) residues. Peptide **1d** displayed alternating chirality (*l*-F_x; *d-pro-pal*), whereas all amino acids in peptide **1e** possessed the natural *l*-chirality. No significant change in subcellular localization was observed for these stereoisomers (**b**); however, the overall cellular uptake of **1e** was greater in HeLa cells after a 60 min incubation (**c**), suggesting that overall stereochemistry of the peptide does play a role in this function.

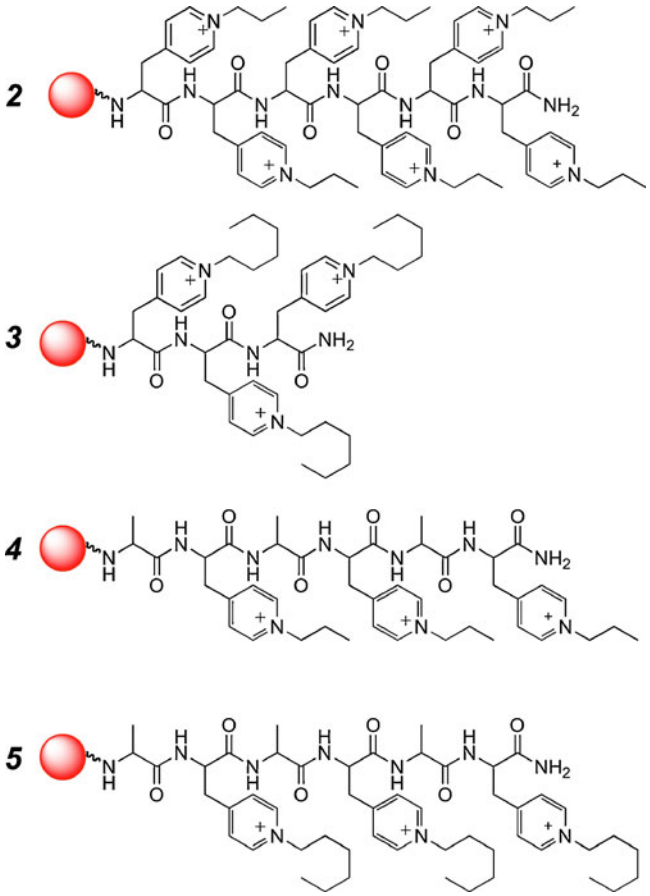

Fig. 7 Schematic of the chemical structures for the polymeric DLC MPPs. For the *pro-pal* polymers, fully synthesized peptides were alkylated with iodopropane (**2** and **4**) or iodohexane (**3** and **5**) while still bound to resin. See Materials and Methods for detailed synthetic protocols. See Supplementary Material for full chemical structures, as well as mass spectrometry and HPLC analysis.

exhibited stronger uptake relative to the analogue that possessed an identical sequence displaying alternating *l*- and *d*- stereochemistry (**1d**) (Fig. 6). Moreover, the cellular uptake of the **4e** approached that of the readily permeable cell-penetrating peptide **tat** (RKKRRQRRR), despite possessing six less positive charges (Fig. 6c). As the retention times of these diastereomers are not equivalent, this implies that the differences are due to distinct apparent hydrophobicities arising from the nearest neighbor effects from the alternative stereochemistry. Since peptide **1e** has a greater apparent hydrophobicity, this likely contributes to the enhanced cellular uptake seen with this molecule. Importantly, the difference in stereochemistry did not affect the subcellular localization profiles of these peptides or the uniform cellular uptake (Fig. 6b and S4). Thus, MPP **1e** exhibits superior properties, with efficient cellular uptake and specific mitochondrial localization relative to all the peptides tested and, therefore, is an optimal design for an MPP.

Synthesis and Evaluation of Polymeric DLC MPPs

In order for cationic peptides to access mitochondria, it is essential that a critical balance of positive charge and lipophilicity be maintained. As the synthetic cationic residues k_π and *pro-pal* possess both lipophilic and cationic character within the side chain moiety, it was hypothesized that these single amino acids could theoretically provide both of the requisite physiochemical properties. Combined with the fact that these amino acids contributed to a more selective mitochondrial localization, a homopolymer of *pro-pal* was designed with a similar length to the MPPs in the previous studies to test whether it could present a simple platform and superior properties for MPPs (Fig. 7).

Synthesis of the polymer was carried out in a similar manner to the alternating hydrophobic/cationic peptides as described previously (Fig. 2b). A peptide containing six pyridyl alanine residues was synthesized and reacted with excess iodopropane, while either still bound to or cleaved from the resin, to afford peptide **2** (Fig. 7). In both solid-phase and solution-phase reactions, complete conversion of the pyridyl groups into the quaternary pyridyl salts was observed. Despite the fact that the side chains displayed lipophilic chains, the relative overall hydrophobicity of **2** was drastically reduced as determined by relative retention times using reverse phase HPLC (Table I), indicating the increase in the number of charged residues dominated this property. As this peptide did not possess the requisite hydrophobicity, no mitochondrial localization was observed for this peptide (Fig. 8). In fact, the punctate fluorescence staining pattern was more similar to that of **tat**, confirming that highly charged peptides lacking

Table I Relative Physiochemical Properties of the Peptide Panel

Peptide	Charge[a]	MW (g/mol)	HPLC elution (%MeCN)[b]
tat	+8	1726.1	35
1a	+3	1247.8	48
1b	+3	1331.8	50
1c	+3	1436.9	50
1d	+3	1436.9	52
1e	+3	1436.9	54
2	+6	1552.0	38
3	+3	1103.7	50
4	+3	1190.6	38
5	+3	1316.8	50

[a] Overall charge of the peptide. Note: As the fluorophore used in these studies was positively charged, this contributed an additional +1 charge to each of the conjugates. [b] Relative hydrophobicities as measured by retention on a reverese-phase HPLC column. See Materials and Methods for the detailed protocol

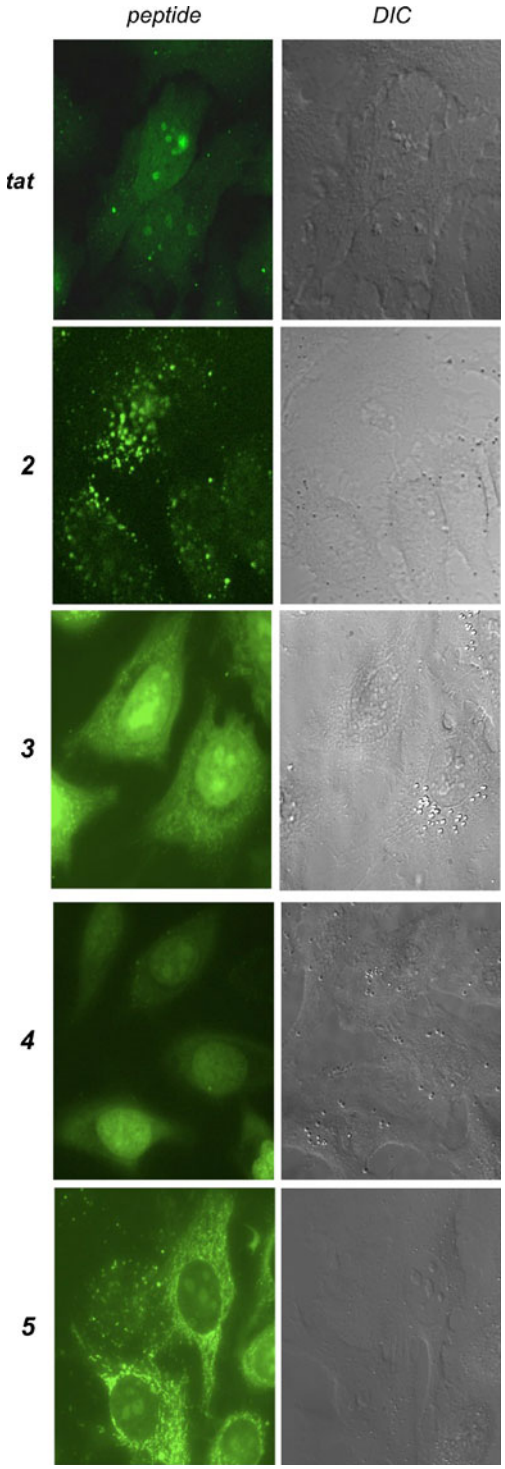

Fig. 8 Subcellular localization of polymeric DLC MPPs. Representative fluorescence microscopy images of HeLa cells acquired with an epifluorescence microscope using 63x objective are shown for the fluorophore-labeled peptide and DIC channels. See Materials and Methods for a detailed protocol.

requisite hydrophobicity are not sufficient as MPPs. In order to restore the hydrophobicity of the polymer, the molecule was redesigned with half the number of charges to reduce hydrophilicity (**3** and **4**). Peptide **3** was designed with longer alkyl chains to further increase the overall lipophilicity, while the structure of **4** offered a control for overall length of the peptide. These peptides were synthesized in a similar manner to **2**, with slight modifications for peptide **3**; in place of a hexamer scaffold and iodopropane, a trimer of pyridyl alanine and the reagent iodohexane was used.

From the retention time of the reverse-phase HPLC column, it is evident that the design of peptide **3** was successful in modulating the lipophilicity, as this molecule displays similar physiochemical parameters to the previous MPPs; however, despite the reduced number of charges, peptide **4** was still significantly less lipophilic, highlighting the importance of the alkyl chain in increasing overall hydrophobicity of these peptides (Table I). Thus, the trimer (**3**) is an ideal molecule to test whether polymers offer an enhanced design for MPPs. Evaluation of the subcellular localization profile in HeLa cells, however, revealed a striking result (Fig. 8). While polymer **2** was clearly below the lipophilicity threshold for mitochondrial localization, polymer **3** was not selective for mitochondria, despite possessing similar charge and hydrophobicity to known MPPs. Instead, this peptide was seen to preferentially localize into the nucleus and cytoplasm of cells.

While many of the physicochemical parameters were kept constant, the overall length of peptide **3** was shorter. As clustering charges was previously seen to prevent access to the mitochondria for MPPs (16), it was important to test whether this limitation was affecting mitochondrial access for polymer **3**. Indeed, when alanine spacers were incorporated into the molecule to control for length (**5**), selective mitochondrial accumulation was restored for this peptide (Fig. 8). It is noteworthy that peptide **4**, with equivalent charge and also displaying alanine spacers, does not exhibit mitochondrial localization, further confirming the rigid lipophilicity thresholds for a cationic peptide to access mitochondria. The results from these studies provide evidence that polymers of the synthetic amino acids with dual properties are not a sufficient platform for a MPP, as the increased charge density overwhelms the lipophilic tails and abrogates access to the mitochondria.

DISCUSSION

Studies of mitochondria-targeted peptides have thus far focused on naturally occurring cationic residues. Here we were able to test whether delocalization of the cationic charge within an amino acid would enhance the properties of MPPs. MPPs displaying these residues, while they exhibited diminished cellular uptake, resulted in slightly

enhanced and more uniform mitochondrial localization. Altering the relative chirality of the peptide importantly restored the strong cellular uptake, as evident from studies comparing the relative internalization efficiencies of a peptide and its diastereomer.

Another important observation made in these studies was the importance of maintaining a global amphipathic character. While deviation from the alternating cationic/hydrophobic amino acid scaffold still resulted in mitochondrial localization of the peptide (16), the overall distribution of the hydrophobic and polar regions was a key factor that directly influenced the mitochondrial localization of these peptides. Through examination of the sequence dependence of MPPs, it was evident that clustering the cationic residues prevented mitochondrial access, even though the peptides had identical amino acid composition. Importantly, the analogs with clustered charges, in fact, exhibited more lipophilic/hydrophobic character by experimental measurements, ruling out the possibility that this property affected subcellular distribution (16). In addition, polymers of the novel cationic amino acids, with side chain moieties comprised of a pyridyl salt and alkyl tail (both positive charge and hydrophobic character) did not localize into the mitochondria, despite possessing requisite hydrophobicity relative to other MPPs. Both of these examples illustrate the importance of evenly distributing the positive charges over the entire molecular scaffold. As charge density has an effect on the ability for these peptides to achieve specific mitochondrial localization, this may indicate that the clustered charges provide an energetic barrier to efficient inner mitochondrial membrane translocation.

CONCLUSION

Understanding the principles behind mitochondrial targeting using MPPs is crucial for engineering an MPP suitable for drug delivery. While it was evident from previous studies that the cationic residues were crucial for MPP cellular uptake and mitochondrial localization, further investigation of the role of the positively charged functional groups allowed for enhancement of highly specific mitochondrial localization. By allowing for an increase in the overall hydrophobicity through charge delocalization, MPPs displayed a more uniform and specific mitochondrial accumulation. In addition, it was found that the ability for the cationic functional group to hydrogen bond increased the peptides overall cellular internalization, supporting previous findings that this is an important interaction that allows for cationic peptides to traverse the plasma membrane. Interestingly, this type of interaction was not needed for crossing mitochondrial membranes, as MPPs displaying the pyridyl salt residues were efficient at achieving mitochondrial localization. Systematic inspection of the chirality of the peptides demonstrated that MPPs with all natural chirality exhibited enhanced cellular uptake compared to diastereomers, while stereochemistry was not observed to affect mitochondrial sequestration of the peptides. These studies provided a greater understanding of the requirements for effective MPPs and led to a second generation of these organelle-specific peptides.

REFERENCES

1. Stewart KM, Horton KL, Kelley SO. Cell-penetrating peptides as delivery vehicles for biology and medicine. Org Biomol Chem. 2008;6:2242–55.
2. Fonseca SB, Pereira MP, Kelley SO. Recent advances in the use of cell-penetrating peptides for medical and biological applications. Adv Drug Deliv Rev. 2009;61(11):953–64.
3. Siprashvili Z, Reuter JA, Khavari PA. Intracellular delivery of functional proteins via decoration with transporter peptides. Mol Ther. 2004;9(5):721–8.
4. Lewin M, Carlesso N, Tung CH, Tang XW, Cory D, Scadden DT, *et al.* Tat peptide-derivatized magnetic nanoparticles allow *in vivo* tracking and recovery of progenitor cells. Nat Biotech. 2000;18(4):410–4.
5. Lindgren M, Rosenthal-Aizman K, Saar K, Eiriksdottir E, Jiang Y, Sassian M, *et al.* Overcoming methotrexate resistance in breast cancer tumour cells by the use of a new cell-penetrating peptide. Biochem Pharmacol. 2006;71(4):416–25.
6. Rothbard JB, Garlington S, Lin Q, Kirschberg T, Kreider E, McGrane PL, *et al.* Conjugation of arginine oligomers to cyclosporin A facilitates topical delivery and inhibition of inflammation. Nat Med. 2000;6:1253–7.
7. Wender PA, Mitchell DJ, Pattabiraman K, Pelkey ET, Steinman L, Rothbard JB. The design, synthesis, and evaluation of molecules that enable or enhance cellular uptake: peptoid molecular transporters. Proc Natl Acad Sci. 2000;97(24):13003–8.
8. Wender PA, Rothbard JB, Jessop TC, Kreider EL, Wylie BL. Oligocarbamate molecular transporters: design, synthesis, and biological evaluation of a new class of transporters for drug delivery. J Am Chem Soc. 2002;124(45):13382–3.
9. Chiu Y-L, Ali A, Chu C-Y, Cao H, Rana TM. Visualizing a correlation between siRNA localization, cellular uptake, and RNAi in living cells. Chem Biol. 2004;11(8):1165–75.
10. Magnus R, Yogesh M, Markus S, Dieter S. Cellular uptake studies with beta-Peptides. ChemBioChem. 2002;3(2–3):257–9.
11. Rothbard JB, Kreider E, VanDeusen CL, Wright L, Wylie BL, Wender PA. Arginine-rich molecular transporters for drug delivery: role of backbone spacing in cellular uptake. J Med Chem. 2002;45(17):3612–8.
12. Bonduelle CV, Gillies ER. Dendritic guanidines as efficient analogues of cell-penetrating peptides. Pharmaceuticals. 2010;3:636–66.
13. Gammon ST, Villalobos VM, Prior JL, Sharma V, Piwnica-Worms D. Quantitative analysis of permeation peptide complexes labeled with technetium-99m: Chiral and sequence-specific effects on net cell uptake. Bioconjug Chem. 2003;14(2):368–76.
14. Zhao K, Zhao G-M, Wu D, Soong Y, Birk AV, Schiller PW, *et al.* Cell-permeable peptide antioxidants targeted to inner mitochondrial membrane inhibit mitochondrial swelling, oxidative cell death, and reperfusion injury. J Biol Chem. 2004;279:34682–90.
15. Horton KL, Stewart KM, Fonseca SB, Guo Q, Kelley SO. Mitochondria-penetrating peptides. Chem Biol. 2008;15(4):375–82.

16. Yousif L, Stewart KM, Horton KL, Kelley SO. Mitochondria-penetrating peptides: sequence effects and model cargo transport. ChemBioChem. 2009;10:2081–8.
17. Fonseca SB, Pereira MP, Mourtada R, Gronda M, Hurren R, Minden MD, *et al.* Re-routing chlorambucil to the mitochondria enhances potency and combats drug resistance in cancer cells. Chem Biol. 2011;18(4):445–53.
18. Pereira M, Kelley SO. Maximizing the therapeutic window of an antimicrobial drug by imparting mitochondrial sequestration in human cells. J Am Chem Soc. 2011;133(10):3260–3.
19. Murphy MP. Targeting lipophilic cations to mitochondria. Biochim Biophys Acta. 2008;1777(7–8):1028–31.
20. Modica-Napolitano JS, Aprille JR. Delocalized lipophilic cations selectively target the mitochondria of carcinoma cells. Adv Drug Deliv Rev. 2001;49:63–70.
21. Johnson LV, Walsh ML, Chen LB. Localization of mitochondria in living cells with rhodamine 123. Proc Natl Acad Sci. 1980;77:990–4.
22. Weissig V, Torchilin VP. Cationic bolasomes with delocalized charge centers as mitochondria-specific DNA delivery systems. Adv Drug Deliv Rev. 2001;49:127–49.
23. Carreon JR, Stewart KM, Mahon KP, Shin S, Kelley SO. Cyanine dye conjugates as probes for cellular imaging. Biorg Med Chem Lett. 2007;17:5182–5.
24. Chen P, Bodor N, Wu W-M, Prokai L. Strategies to target kyotorphin analogues to the brain. J Med Chem. 1998;41 (20):3773–81.
25. Bodor N, Toth-Sarudy E, Holm T, Pallagi I, Vass E, Buchwalk P, *et al.* Novel, cell-penetrating molecular transporters with flexible backbones and permanently charged side-chains. J Pharm Pharmacol. 2007;59:1065–76.
26. Honig BH, Hubbell WL, Flewelling RF. Electrostatic interactions in membranes and proteins. Annu Rev Biophys Biophys Chem. 1986;15(1):163–93.
27. Mitchell DJ, Steinman L, Kim DT, Fathman CG, Rothbard JB. Polyarginine enters cells more efficiently than other polycationic homopolymers. J Pept Res. 2000;56(5):318–25.
28. Katayama S, Hirose H, Takayama K, Nakase I, Futaki S. Acylation of octaarginine: implication to the use of intracellular delivery vectors. J Control Release. 2011;149(1):29–35.
29. Poon GMK, Gariepy J. Cell-surface proteoglycans as molecular portals for cationic peptide and polymer entry into cells. Biochem Soc Trans. 2007;35:788–93.
30. Richard JP, Melikov K, Brooks H, Prevot P, Lebleu B, Chernomordik LV. Cellular uptake of unconjugated TAT peptide involves clathrin-dependent endocytosis and heparan sulfate receptors. J Biol Chem. 2005;280(15):15300–6.
31. Nakase I, Tadokoro A, Kawabata N, Takeuchi T, Katoh H, Hiramoto K, *et al.* Interation of arginine-rich peptides with membrane-associated proteoglycans is curicial for induction of actin organization and macropinocytosis. Biochemistry. 2007;46:492–501.
32. Ziegler A, Nervi P, Durrenberger M, Seelig J. The cationic cell-penetrating peptide CPP(Tat) derived from the HIV-1 protein TAT is rapidly transported into living fibroblasts: optical, biophysical, and metabolic evidence. Biochemistry. 2005;44:138–48.